

Self-induced transmission on intersubband resonance in multiple quantum wellsNi Cui,^{1,2} Yueping Niu,¹ Hui Sun,^{1,2} and Shangqing Gong^{1,*}¹*State Key Laboratory of High Field Laser Physics, Shanghai Institute of Optics and Fine Mechanics, Chinese Academy of Sciences, Shanghai 201800, China*²*Graduate University of Chinese Academy of Sciences, Beijing 100049, China*

(Received 20 December 2007; revised manuscript received 11 June 2008; published 26 August 2008)

We investigate the nonlinear propagation of ultrashort pulses on resonant intersubband transitions in multiple semiconductor quantum wells. It is shown that the nonlinearity rooted from electron-electron interactions destroys the condition giving rise to self-induced transparency. However, by adjusting the area of input pulse, we find the signatures of self-induced transmission due to a full Rabi flopping of the electron density, and this phenomenon can be approximately interpreted by the traditional standard area theorem via defining the effective area of input pulse.

DOI: [10.1103/PhysRevB.78.075323](https://doi.org/10.1103/PhysRevB.78.075323)

PACS number(s): 42.50.Md, 78.47.-p, 78.20.Bh, 78.67.-n

I. INTRODUCTION

The nonlinear propagation of ultrashort laser pulses through multiple quantum wells (QWs) has attracted tremendous interests¹⁻⁸ for a broad range of both science and technical application, which is particularly crucial for the understanding of coherent nonlinear light-matter interaction. It is well known that (different from atomic systems which can be modeled by noninteracting two-level systems⁹) the optical effects in semiconductors have been substantially modified due to the Coulomb interaction between optically generated electron-hole excitations.¹⁰ In particular, the many-body effects arising from the macroscopic carrier density on free-exciton resonances in condensed matter¹¹ may prevent the establishment of complete self-induced transparency (SIT) according to the area theorem.^{12,13} Nevertheless, Rabi flopping of the carrier density, coherent nonlinear long-distance propagation, and a high degree of transmission have been predicted and this so-called self-induced transmission phenomenon has been observed in bulk CdSe (Refs. 14 and 15) and in a multiple quantum-well Bragg structure.^{6,7} Moreover, for a multiple QWs structure—except for the many-body effects—the strong radiative coupling effects can dominate the optical properties of the system via the re-emitted field¹ such as a pronounced self-induced absorption⁸ and a large impact on Rabi oscillations of subband populations.¹⁷ The strength of the radiative coupling can be significantly influenced by varying the carrier density as well as the many-body effects.

Recently, coherent nonlinear optical phenomena in intersubband (IS) transitions in semiconductor QWs such as Rabi oscillations,¹⁶⁻¹⁹ Fano interference,^{20,21} electronmagnetically induced transparency,^{22,23} resonant harmonic generation,^{24,25} and nonlinear coherent control has attracted wide attention.²⁶⁻²⁸ It should be emphasized that, in most of these studies, the atomiclike multilevel theoretical approaches have been used for the description of the dynamics of the IS transitions. In particular, for a structure of modulation-doped symmetric double QWs with two electronic subbands coupled by an intense laser field, Olaya-Castro *et al.*²⁹ derived the effective Bloch equations describing the effect of electron-electron interactions on IS transitions for a two-

level system familiar from the atomic physics⁹ and the nonlinearity arising from the macroscopic number of carriers translated into the nonlinear differential equations. Later, by using the effective nonlinear Bloch equations, Paspalakis *et al.*^{18,30} studied the electron dynamics in a symmetric double quantum well with the two-subband approximation and presented the conditions leading to complete population inversion and complete Rabi oscillations, respectively. To the best of our knowledge, no work has been devoted yet to the study of the impact of electron-electron interactions on pulse propagation on resonant IS transitions in such multiple symmetric double QWs.

In the present paper, we investigate the nonlinear propagation of ultrashort pulses on resonant IS transitions in multiple symmetric double QWs by solving the Maxwell's wave equations and the effective nonlinear Bloch equations of Olaya-Castro *et al.*²⁹ Due to the effect of electron-electron interactions, the temporal and spectral properties of transmitted pulses are sensitive to the electron sheet density. The nonlinearity arising from the macroscopic number of electrons destroys the condition leading to SIT. However, by varying the input pulse areas, we find the phenomenon of the self-induced transmission indicating the full Rabi flopping of the electron density. In addition, we can use the standard area theorem to explain the occurrence of self-induced transmission by defining the effective area of input pulse.

II. MODEL AND BASIC EQUATIONS

We consider a n -type modulation-doped multiple QWs sample consisting of N equally spaced electronically uncoupled symmetric double semiconductor GaAs/AlGaAs QWs with separation d as shown in Fig. 1. There are only two lower energy subbands that contribute to the system dynamics; $n=0$ for the lowest subband with even parity and $n=1$ for the excited subband with odd parity. The Fermi level is below the $n=1$ subband minimum, so the excited subband is initially empty. This is succeeded by a proper choice of the electron sheet density. The system dynamics is described by the following effective nonlinear Bloch equations²⁹ when the two subbands are coupled by a time-dependent p -polarized pulse $E(t)$ along the growth direction (z' axis):

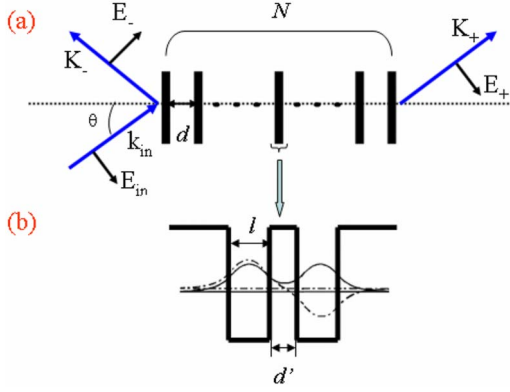


FIG. 1. (Color online) Schematic picture of the model configuration. (a) Multiple quantum-well system consists of $N=50$ periods of double symmetric QWs separated by $d=20$ nm AlGaAs barrier, which is excited by a p -polarized external electric field E_{in} at an angle of incidence θ . E_+ and E_- denote the right and left propagating total outgoing fields, respectively. (b) The structure of each pair of QWs, which comprises double $l=5.5$ nm symmetric GaAs wells coupled through a $d'=1.1$ nm AlGaAs barrier. The solid and dotted lines represent the lowest and excited subbands, respectively.

$$\partial_t S_1(t) = [\omega_{10} - \gamma S_3(t)] S_2(t) - \frac{S_1(t)}{T_2}, \quad (1)$$

$$\partial_t S_2(t) = -[\omega_{10} - \gamma S_3(t)] S_1(t) + 2 \left[\frac{\wp E(t)}{\hbar} - \beta S_1(t) \right] S_3(t) - \frac{S_2(t)}{T_2}, \quad (2)$$

$$\partial_t S_3(t) = -2 \left[\frac{\wp E(t)}{\hbar} - \beta S_1(t) \right] S_2(t) - \frac{S_3(t) + 1}{T_1}. \quad (3)$$

Here, $S_1(t)$ and $S_2(t)$ are, respectively, the mean real and imaginary parts of polarization and $S_3(t)$ is the mean population inversion per electron (the difference of the occupation probabilities in the upper and lower subbands). \wp is the electric dipole matrix element between the two subbands and N_v is the electron volume density. Also, the nonlinear parameters $\omega_{10}, \beta, \gamma$ are given by

$$\omega_{10} = \frac{E_1 - E_0}{\hbar} + \frac{\pi e^2}{\hbar \epsilon_r} N_s \frac{L_{1111} - L_{0000}}{2}, \quad (4)$$

$$\gamma = \frac{\pi e^2}{\hbar \epsilon_r} N_s \left(L_{1001} - \frac{L_{1111} + L_{0000}}{2} \right), \quad (5)$$

$$\beta = \frac{\pi e^2}{\hbar \epsilon_r} N_s L_{1100}. \quad (6)$$

Here, ω_{10} is the renormalized but time-independent transition energy, β is the coefficient of the nonlinear term that renormalizes the applied field due to induced polarization, and γ is a result of the interplay between vertex and self-energy corrections to the transition energy. The depolarization effects parameters γ and β are traced from the nonlinearity arising

from electron-electron interactions on IS transitions in semiconductor QWs. N_s is the electron sheet density, ϵ_r is the relative dielectric constants, e is the electron charge, E_0, E_1 are the eigenvalues of energy for the ground and excited states in the well, respectively, and $L_{ijkl} = \iint dz' dz'' \xi_i(z') \xi_j(z'') |z' - z''| \xi_k(z'') \xi_l(z')$ with $i, j, k, l = 0, 1$. Also, $\xi_i(z')$ is the wave function for the i th subband along the growth direction (z' axis). In Eqs. (1)–(3) the terms containing the population decay T_1 and the dephasing T_2 times describe relaxation processes in the quantum well and have been added phenomenologically in the effective nonlinear Bloch equations. However, the issue of relaxation is a difficult one and is closely related to the extension of the proposed wave function to include correlations and the interaction with phonons. If there is no relaxation in the system $T_1, T_2 \rightarrow \infty$ then $S_1^2(t) + S_2^2(t) + S_3(t) = 1$.

We investigate the propagation property of an ultrashort laser pulse $E_x(z, t)$ along the z axis in the multiple double symmetric QWs. With the constitute relation for the electric displacement for the polarization along the x axis, the Maxwell's wave equation for the medium takes the form

$$\partial_t H_y = -\frac{1}{\mu} \partial_z E_x, \quad (7)$$

$$\partial_t E_x = -\frac{1}{\epsilon} \partial_z H_y - \frac{1}{\epsilon} \partial_t P_x, \quad (8)$$

where E_x, H_y are the electric and magnetic fields, respectively, while ϵ and μ are the electric permittivity and the magnetic permeability in the medium, respectively. In Refs. 17 and 20, we consider transverse magnetic polarized pulses incident at an angle $\theta=45^\circ$ with respect to the growth axis (z' axis) so that the transition dipole moment \wp includes a factor $1/\sqrt{2}$ as intersubband transitions are polarized along the growth axis. The macroscopic nonlinear polarization $P_x = -N_v S_1(t) \wp / \sqrt{2}$ is connected to the off-diagonal density-matrix element $S_1(t), S_2(t)$ and the population difference $S_3(t)$ between the subbands, which is determined by the effective nonlinear Bloch equations [Eqs. (1)–(3)] with the dipole moment \wp , changes to $\wp / \sqrt{2}$.

III. SELF-INDUCED TRANSMISSION ON INTERSUBBAND RESONANCE

In this section, we will discuss the nonlinear propagation of the ultrashort pulses on resonant IS transitions in multiple GaAs/AlGaAs symmetric double QWs on the basis of the numerical solutions of the full wave Maxwell-Bloch equations [Eqs. (1)–(3), (7), and (8)]. The structure of the multiple QWs contains $N=50$ equally spaced double symmetric QWs with separation $d=20$ nm Al_{0.267}Ga_{0.733}As barrier as shown in Fig. 1(a). Each pair of QWs [Fig. 1(b)] consists of two GaAs symmetric square wells with 5.5 nm width and 219 meV height coupled by a $d'=1.1$ nm Al_{0.267}Ga_{0.733}As barrier as shown in Fig. 1(a). Then, the system parameters, which are dependent on the electron sheet density N_s , can be calculated. For example, the electron sheet density is taken to be $N_s = 1.0 \times 10^{11}$ cm⁻² and the electron volume density is

$N_v = N_s/L$, where L is the width of the period of the multiple QWs. Then the parameters are calculated to be $E_1 - E_0 = 44.955$ meV, $\pi e^2 N_s (L_{1111} - L_{0000}) / 2\epsilon_r = 0.206$ meV, $\hbar\gamma = 0.0475$ meV, and $\hbar\beta = -0.78$ meV. The dipole moment for the structure is $\varphi = -32.9e$ Å and the relative dielectric constant is $\epsilon_r = 12$. In addition, as the dephasing is the crucial relaxation process in semiconductor QWs, we choose $T_1 = 100$ ps and $T_2 = 10$ ps as in Ref. 30.

The full Maxwell-Bloch equations [Eqs. (1)–(3), (7), and (8)] are solved by using the iterative predictor-corrector finite-difference time-domain method.^{31–33} In what follows, we assume that the system is initially in the lowest subband so the initial conditions are $S_1(0) = S_2(0) = 0$ and the population difference is $S_3(0) = -1$. We consider a hyperbolic secant functional form for the initial incident pulse, which is described by

$$E_x(z=0, t) = \mathcal{E}_0 \operatorname{sech}[1.76(t - t_0)/\tau_p] \cos[\omega_p(t - t_0)], \quad (9)$$

where \mathcal{E}_0 is the electric-field amplitude and ω_p is the central carrier frequency. The coefficient 1.76 is used to adjust the definition of the full width at half maximum (FWHM) of the pulse intensity envelope of the laser pulse to the definition of pulse duration; in this condition, τ_p is the FWHM and t_0 is the delay. The system we consider is excited at exact resonance $\omega_p = \omega_{10}$ and the duration of the applied pulse is $\tau_p = 0.2$ ps. For the following application, we characterize the strength of the electron-light interactions by the input pulse area $\Theta(z=0) = \int_{-\infty}^{\infty} \frac{\varphi\sqrt{2}}{\hbar} E_x(z=0, t') dt' = \Omega_0 \tau_p \pi / 1.76$, where $\Omega_0 = -(\varphi/\sqrt{2})\mathcal{E}_0/\hbar$ is the peak of the Rabi frequency.

The numerical result of 2π ultrashort laser pulses propagating in resonant two-subband multiple QWs with different electron sheet densities is depicted in Fig. 2. It is shown that the change in sheet density N_s leads to distinctly different behaviors of the transmitted pulses. For much smaller sheet density $N_s = 0.5 \times 10^{11}$ cm⁻², the multiple QWs structure seems to be approximately transparent to the 2π pulses [Fig. 2(b)] and the corresponding spectrum [Fig. 2(f)] has basically no change compared to the input spectrum [Fig. 2(e)]. Accordingly, there is a full Rabi flopping of the electron population difference within the IS transitions in each double QWs as shown in Fig. 3(a). Therefore, the phenomenon of SIT is approximately reproduced with minor modifications. For larger electron sheet densities, $N_s = 5 \times 10^{11}$ cm⁻² and $N_s = 8 \times 10^{11}$ cm⁻², there is a visible broadening in temporal pulses and even pulse breakup for further larger N_s [Fig. 2(d)]. The corresponding normalized spectra are obviously suppressed [Figs. 2(g) and 2(h)] and even a significant breakup in the spectrum in Fig. 2(h). Simultaneously, the full Rabi flopping in each double QWs is not possible especially in the frontier of QWs structure as shown in Figs. 3(b) and 3(c). It means that the increase in electron sheet density prevents the establishment of complete SIT in multiple QWs structure due to strong electron-electron interactions.

The physical mechanism of the above phenomenon can be understood as follows. The presence of the nonlinear parameters γ and β , which depend directly on the electron sheet density N_s [Eqs. (5) and (6)], makes the effective Bloch equations [Eqs. (1)–(3)] for the symmetric double QWs dif-

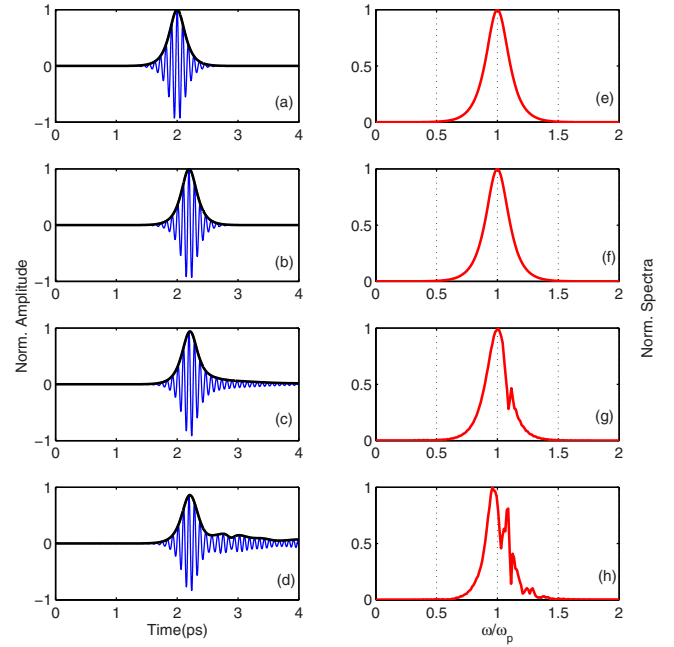


FIG. 2. (Color online) (a)–(d) The propagation of 2π pulses through the multiple QWs structure for different electron sheet densities. (a) The input pulse for (b) $N_s = 0.5 \times 10^{11}$ cm⁻², (c) $N_s = 5 \times 10^{11}$ cm⁻², and (d) $N_s = 8 \times 10^{11}$ cm⁻². The black thick curves represent the pulse envelopes. (e)–(h) are the normalized spectra corresponding to (a)–(d), respectively.

ferent from the two-level atom systems.^{9,12,13} For small N_s , the contributions of γ and β can be neglected compared to Rabi frequencies. However, for larger N_s , γ and β become comparable to Rabi frequency Ω_0 , which introduces time dependence of the transition energy and effective Rabi frequency. γ induces time-dependent effective transition energies of the electrons and β yields an internal field due to induced polarization, which renormalizes the Rabi frequency. Therefore, the renormalized Rabi frequency depends on the IS coherence which is driven by the incident field, i.e., not only on time, but also on laser frequency and pulse duration of the incident field. The transition energy that varies with time induces a second time-dependent renormalization of the effective Rabi frequency. In addition, due to the modification of radiative coupling effects, which is also dependent on carrier density, the local electric field in the structure is not equal to the incident field and exhibits strong temporal and spatial dependences. Therefore, the increase in the electron sheet density makes the parameters γ , β and other nonlinear responses such as radiative coupling become larger, thus leading to the disappearance of the phenomenon of SIT.

However, for the larger sheet density, by varying the input pulse areas $\Theta(z=0)$ for $N_s = 5 \times 10^{11}$ cm⁻² at $\Theta(z=0) = 2.24\pi$ [Fig. 4(b)] and for $N_s = 8 \times 10^{11}$ cm⁻² at $\Theta(z=0) = 2.57\pi$ [Fig. 4(c)], the pulses transmit the structure essentially unaltered with respect to the input pulses, presuming that we neglect a decrease in pulse envelope and a slight broadening induced by the dispersion. The corresponding spectra do not differ significantly from the input spectrum [Figs. 4(e) and 4(f)]. This phenomenon of self-induced transmission in semiconductors does occur, which indicates that a

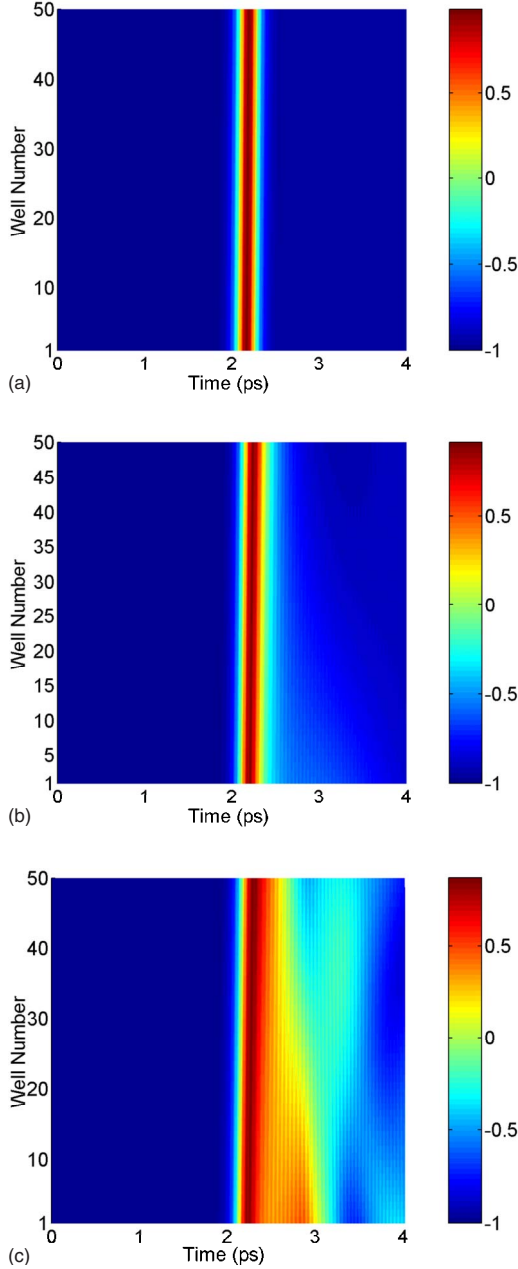


FIG. 3. (Color online) The time evolution of the population difference $S_3(t)$ in each double QWs for different electron sheet densities (a) $N_s=0.5 \times 10^{11} \text{ cm}^{-2}$, (b) $N_s=5 \times 10^{11} \text{ cm}^{-2}$, and (c) $N_s=8 \times 10^{11} \text{ cm}^{-2}$.

full Rabi flopping of the electron density has occurred within the IS transitions of each double QWs.

Furthermore, we present the dependence of the input pulse area $\Theta(z=0)$ for the occurrence of self-induced transmission on the electron sheet density in Fig. 5 with the triangles. The values of N_s , which is taken up in numerical simulations, satisfy the system initial conditions that the Fermi energy is smaller than the excited subband energy, i.e., the system is in the ground subband initially. It is shown that the area of input pulse depends directly on the electron sheet density. For small sheet densities [$N_s \leq 1.0 \times 10^{11} \text{ cm}^{-2}$], the effects of electron-electron interaction are so small that the

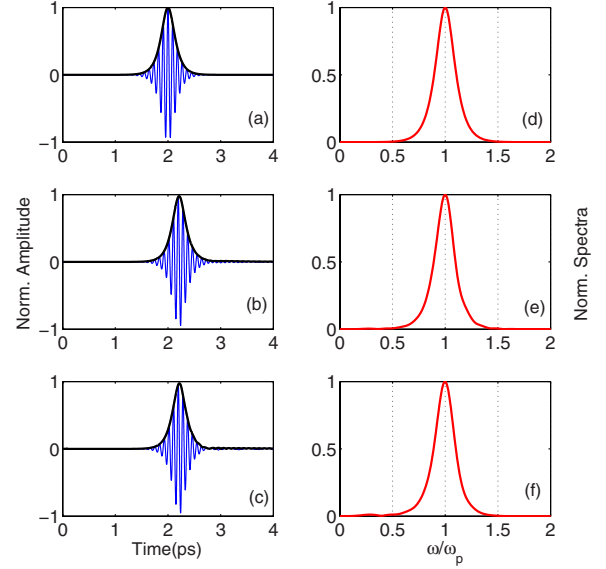


FIG. 4. (Color online) Normalized amplitude (thin blue curve) of the input pulse versus time (a) and the transmitted pulses for different electron sheet densities with different input pulse area versus time; (b) $N_s=5 \times 10^{11} \text{ cm}^{-2}$, $\Theta(z=0)=2.24\pi$ and (c) $N_s=8 \times 10^{11} \text{ cm}^{-2}$, $\Theta(z=0)=2.57\pi$. The black thick curves represent the pulse envelopes. (d)–(f) are the normalized spectra corresponding to (a)–(c), respectively.

quantum-well structure equivalents to a noninteracting two-level atom system in which 2π pulses can propagate without suffering significant losses according to the area theorem. While, the increase in the electron sheet density destroys the condition leading to SIT. The area of input pulse for the occurrence of self-induced transmission increases with the increasing electron density synchronously and is always larger than 2π . Nevertheless, combining with the nonlinear parameters γ and β , we define an effective area of input pulse according to Ref. 30; $\Theta_{\text{eff}}^2(z=0) = \Theta^2(z=0) - 2[(\gamma - \beta)\tau_p\pi/1.76]^2$, i.e., an effective coupling of light matter. In spite the electron sheet density of QWs and the input pulse area vary in a relative large range, the effective pulse area $\Theta_{\text{eff}}(z=0)$ for the occurrence of self-induced transmission keeps an invariant area of 2π as shown

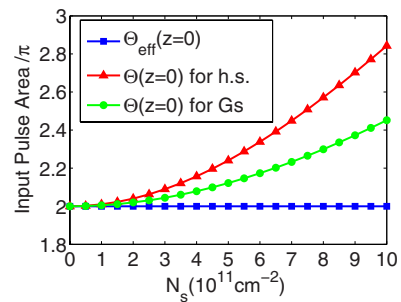


FIG. 5. (Color online) The input pulse area $\Theta(z=0)$ and the effective area $\Theta_{\text{eff}}(z=0)$ (squares) for the occurrence of self-induced transmission as a function of the electron sheet densities N_s . The triangles are for hyperbolic secant pulses (h.s.) and the circles are for Gaussian pulses (Gs). The lines are guides to the eyes.

in Fig. 5 with squares. Considering both Figs. 4 and 5 and assuming that we neglect the decrease in the area of transmitted pulses, the phenomenon of self-induced transmission can be approximately explained by traditional standard area theorem with the effective area of input pulses.

In addition, we have also investigated the propagation properties of Gaussian pulses in the multiple QWs systems. With the same pulse duration and the central carrier frequency above, we have also found the phenomenon of self-induced transmission with Gaussian pulses. The input pulse areas $\Theta(z=0)$ for the occurrence of self-induced transmission with different electron sheet densities are shown in Fig. 5 with circles. Therefore, the feasibility for the occurrence of self-induced transmission on resonant IS transitions in multiple symmetric double semiconductor QWs can be clearly determined, which is useful to achieve a high degree of transmission for this structure.

IV. CONCLUSIONS

In conclusion, we have investigated the nonlinear propagation of ultrashort pulses on resonant IS transitions in multiple GaAs/AlGaAs symmetric double QWs by solving the Maxwell-Bloch equations. Numerical simulations have re-

vealed that the increase in the carrier densities leads to the strong nonlinearities rooted from the macroscopic number of electrons in QWs, which reduces the feasibility for the establishment of SIT. However, by adjusting the area of input pulses, we found the phenomenon of self-induced transmission, which can be approximately explained by the traditional area theorem via defining the effective area of input pulses in spite the electron density varies in a relative large range. This approach would be beneficial to achieve a high degree of transmission for a structure of multiple double semiconductor QWs.

ACKNOWLEDGMENTS

We are sincerely grateful to E. Paspalakis and A. Olaya-Castro for their useful discussions. This work is supported by the National Natural Sciences Foundation of China with Grants No. 60708008 and No. 60578050, the Project of Academic Leaders in Shanghai with Grant No. 07XD14030, the Shanghai Commission of Science and Technology with Grant No. 06DZ22015, 0652 nm005, the National Basic Research Program of China (973 Program) with Grant No. 2006CB921104, and by the Knowledge Innovation Program of the Chinese Academy of Sciences.

*Corresponding author; sqgong@mail.siom.ac.cn

- ¹T. Stroucken, A. Knorr, P. Thomas, and S. W. Koch, Phys. Rev. B **53**, 2026 (1996).
- ²M. Hübner, J. Kuhl, T. Stroucken, A. Knorr, S. W. Koch, R. Hey, and K. Ploog, Phys. Rev. Lett. **76**, 4199 (1996).
- ³S. Haas, T. Stroucken, M. Hübner, J. Kuhl, B. Grote, A. Knorr, F. Jahnke, S. W. Koch, R. Hey, and K. Ploog, Phys. Rev. B **57**, 14860 (1998).
- ⁴J. P. Prineas, C. Ell, E. S. Lee, G. Khitrova, H. M. Gibbs, and S. W. Koch, Phys. Rev. B **61**, 13863 (2000).
- ⁵M. Schaarschmidt, J. Förstner, A. Knorr, J. P. Prineas, N. C. Nielsen, J. Kuhl, G. Khitrova, H. M. Gibbs, H. Giessen, and S. W. Koch, Phys. Rev. B **70**, 233302 (2004).
- ⁶N. C. Nielsen, J. Kuhl, M. Schaarschmidt, J. Förstner, A. Knorr, S. W. Koch, G. Khitrova, H. M. Gibbs, and H. Giessen, Phys. Rev. B **70**, 075306 (2004).
- ⁷T. H. zu Siederdisen, N. C. Nielsen, J. Kuhl, M. Schaarschmidt, J. Förstner, A. Knorr, G. Khitrova, H. M. Gibbs, S. W. Koch, and H. Giessen, Opt. Lett. **30**, 1384 (2005).
- ⁸T. Shih, K. Reimann, M. Woerner, T. Elsaesser, I. Waldmüller, A. Knorr, R. Hey, and K. H. Ploog, Phys. Rev. B **72**, 195338 (2005).
- ⁹L. Allen and J. H. Eberly, *Optical Resonance and Two-Level Atoms* (Academic, New York/Dover, New York, 1987).
- ¹⁰H. Haug and S. W. Koch, *Quantum Theory of the Optical and Electronic Properties of Semiconductors* (World Scientific, Singapore, 1993).
- ¹¹A. Knorr, R. Binder, M. Lindberg, and S. W. Koch, Phys. Rev. A **46**, 7179 (1992).
- ¹²S. L. McCall and E. L. Hahn, Phys. Rev. Lett. **18**, 908 (1967); Phys. Rev. **183**, 457 (1969).
- ¹³R. W. Ziolkowski, J. M. Arnold, and D. M. Gogny, Phys. Rev. A **52**, 3082 (1995).
- ¹⁴H. Giessen, A. Knorr, S. Haas, S. W. Koch, S. Linden, J. Kuhl, M. Hetterich, M. Grün, and C. Klingshirn, Phys. Rev. Lett. **81**, 4260 (1998).
- ¹⁵N. C. Nielsen, S. Linden, J. Kuhl, J. Förstner, A. Knorr, S. W. Koch, and H. Giessen, Phys. Rev. B **64**, 245202 (2001).
- ¹⁶C. W. Luo, K. Reimann, M. Woerner, T. Elsaesser, R. Hey, and K. H. Ploog, Phys. Rev. Lett. **92**, 047402 (2004).
- ¹⁷I. Waldmüller, W. W. Chow, and A. Knorr, Phys. Rev. B **73**, 035433 (2006).
- ¹⁸E. Paspalakis, M. Tsousidou, and A. F. Terzis, J. Appl. Phys. **100**, 044312 (2006).
- ¹⁹A. A. Batista and D. S. Citrin, Phys. Rev. Lett. **92**, 127404 (2004); Phys. Rev. B **74**, 195318 (2006).
- ²⁰J. H. Wu, J. Y. Gao, J. H. Xu, L. Silvestri, M. Artoni, G. C. La Rocca, and F. Bassani, Phys. Rev. Lett. **95**, 057401 (2005); Phys. Rev. A **73**, 053818 (2006).
- ²¹H. Sun, S. Q. Gong, Y. P. Niu, S. Q. Jin, R. X. Li, and Z. Z. Xu, Phys. Rev. B **74**, 155314 (2006).
- ²²S. M. Sadeghi, J. F. Young, and J. Meyer, Phys. Rev. B **51**, 13349 (1995).
- ²³G. B. Serapiglia, E. Paspalakis, C. Sirtori, K. L. Vodopyanov, and C. C. Phillips, Phys. Rev. Lett. **84**, 1019 (2000).
- ²⁴E. Rosencher and Ph. Bois, Phys. Rev. B **44**, 11315 (1991).
- ²⁵J. N. Heyman, K. Craig, B. Galdrikian, M. S. Sherwin, K. Campman, P. F. Hopkins, S. Fafard, and A. C. Gossard, Phys. Rev. Lett. **72**, 2183 (1994).
- ²⁶X. D. Hu and W. Pötz, Appl. Phys. Lett. **73**, 876 (1998).
- ²⁷T. Müller, W. Parz, G. Strasser, and K. Unterrainer, Phys. Rev. B **70**, 155324 (2004).

- ²⁸M. D. Frogley, J. F. Dynes, M. Beck, J. Faist, and C. C. Phillips, *Nat. Mater.* **5**, 175 (2006).
- ²⁹A. Olaya-Castro, M. Korkusinski, P. Hawrylak, and M. Y. Ivanov, *Phys. Rev. B* **68**, 155305 (2003).
- ³⁰E. Paspalakis, M. Tsaousidou, and A. F. Terzis, *Phys. Rev. B* **73**, 125344 (2006).
- ³¹K. S. Yee, *IEEE Trans. Antennas Propag.* **14**, 302 (1966).
- ³²G. Mur, *IEEE Trans. Electromagn. Compat.* **EMC-23**, 377 (1981).
- ³³A. Taflove and M. E. Brodwin, *IEEE Trans. Microwave Theory Tech.* **23**, 623 (1975).